Creating a Comprehensive Research Platform for Surgical Technique and Operative Outcome in Primary Brain Tumor Neurosurgery

Alexander Winkler-Schwartz[1], Recai Yilmaz[1], Dan Huy Tran[1], Houssem-Eddine Gueziri[3], Binbin Ying[2], Marius Tuznik[4], Vladimir Fonov[3], Louis Collins[3], David A. Rudko[4-6], Jianyu Li[2], Patricia Debergue[7], Valerie Pazos[7], Rolando Del Maestro[1]

BACKGROUND: **The operative environment poses many challenges to studying the relationship between surgical acts and patient outcomes in intracranial oncological neurosurgery. We sought to develop a framework in which neurosurgical performance and extent of resection could be precisely quantified in a controlled setting.**

METHODS: **The stiffness of an alginate hydrogel-based tumor was modified with differing concentrations of the cross-linking agent calcium sulfate until biomechanical properties similar to those of human primary brain tumors measured at resection were achieved. The artificial tumor was subsequently incorporated into an ex-vivo animal brain as a final model. Magnetic resonance imaging enhancement and ultraviolet fluorescence was achieved by incorporating gadolinium and fluorescein solution, respectively. Video recordings from the operative microscope, ceiling cameras, and instrument-mounted fiducial markers within a surgical suite environment captured operative performance.**

RESULTS: **A total of 24 rheometer measurements were conducted on alginate hydrogels containing 10-, 11-, and 12-mM concentrations of calcium sulfate. Sixty-eight stiffness measurements were conducted on eight patient tumor samples. No differences were found between the alginate and brain tumor stiffness values [Kruskal-Wallis $\chi^2(4) = 9.187$; $P = 0.057$]. Tumor was identified using ultraviolet fluorescence and ultrasonography. The volume and location of the resected white and gray matter and residual tumor could be quantified in 0.003-mm^3 increments using a 7T magnetic resonance imaging coil. Ultrasonic aspirator and bipolar electrocautery movement data were successfully transformed into performance metrics.**

CONCLUSION: **The developed framework can offer clinicians, learners, and researchers the ability to perform operative rehearsal, teaching, and studies involving brain tumor surgery in a controlled laboratory environment and represents a crucial step in the understanding and training of expertise in neurosurgery.**

INTRODUCTION

The removal of brain tumors, a skill expected of neurosurgical graduates, confers significant risk to patients and remains among the most technically challenging procedures within medicine. Little more than anecdotal accounts exist of the most effective methods of teaching oncological neurosurgery.

A research framework relating technical performance to operative outcomes in oncological neurosurgery is key to answering questions relating to the training of neurosurgeons and the examination of operative techniques and technologies. Such a framework must account for tumor variability, ensure an adequate method of capturing operative performance in real time, and have

Key words
- Alginate
- Assessment
- Brain neoplasm
- Hydrogel
- Imaging
- Simulation

Abbreviations and Acronyms
3D: 3-Dimensional
MRI: Magnetic resonance imaging

From the [1]Neurosurgical Simulation and Artificial Intelligence Learning Centre and [2]Department of Mechanical Engineering; [3]Neuro Imaging and Surgical Technologies Laboratory, [4]Department of Neurology/Neurosurgery, [5]Quantitative Microstructure Imaging Laboratory, and [6]Department of Biomedical Engineering, McConnell Brain Imaging Centre, Montreal Neurological Institute, McGill University, Montreal; and [7]National Research Council of Canada, Boucherville, Quebec, Canada

To whom correspondence should be addressed: Alexander Winkler-Schwartz, M.D. [E-mail: manuscriptinquiry@gmail.com]

Citation: World Neurosurg. (2020) 144:e62-e71.
https://doi.org/10.1016/j.wneu.2020.07.209

*Journal homepage: **www.journals.elsevier.com/world-neurosurgery***

*Available online: **www.sciencedirect.com***

an accurate method of evaluating operative outcome. However, such a platform does not yet exist.

The influence of a single surgeon's technical performance on operative outcomes can be best understood by creating a convincing operative mimic of a brain tumor surgical procedure that controls for tumor size, tumor location, tumor stiffness, bleeding, and environmental factors. Such a mimic in a standardized operating room would represent an ideal setting to conduct interventional experiments and obviate patient safety concerns.

Little effort has been made to re-create the known tactile and imaging properties of human brain tumors when creating artificial mimics. Various substances have served as artificial brain tumors, including fibrin glue,[1] silicone,[2,3] polymer resins,[4-6] food-grade gels,[7-9] autologous animal organs,[10] and polyvinyl alcohol.[11-13] Although investigators have described the imaging[11,14,15] and biomechanical properties[16] of these artificial tumors, none have explicitly developed tumors using real human brain tumors as the reference standard. None have offered a platform designed to re-create a human brain tumor operative experience with the inclusion of a method to capture and quantify the operative performance relative to the extent of resection.

Alginate hydrogels are polymers derived from algae whose biomedical applications have been expanding,[17] including in drug delivery,[18] as wound dressings, and in tissue engineering.[19] These polymers, although initially liquid-like, can form solid hydrated materials that can be adjusted to the required stiffness at room temperature by varying the concentration of ionic cross-linking agents. These polymers are biocompatible and are ideal substances to inject into ex-vivo or in-vivo tissues, including the brain. Compared with fibrin glue and agarose gels, alginate hydrogels feature an enhanced capacity to develop appropriate stiffness and mechanical toughness for various applications.[17] Moreover, alginate hydrogels exhibit viscoelastic behavior similar to that of brain tissues.[20] Furthermore, unlike polyvinyl alcohol, the desired stiffness can be accomplished in mild conditions without the need for freeze–thaw cycles.

We sought to develop a framework in which surgical performance and the extent of resection could be precisely quantified. This was accomplished by creating an artificial brain tumor using an alginate hydrogel incorporated into an animal brain with biomechanical and imaging characteristics similar to those of human brain tumors. This allowed for accurate pre- and postoperative magnetic resonance imaging (MRI) and ultrasound-based imaging. Operative performance was captured via video recordings from the operative microscope, ceiling mounted cameras, and instrument-mounted fiducial markers within a surgical environment.

METHODS

Establishing Biomechanical Properties of Human Primary Brain Tumors

Human tumor biomechanical characterization was performed using a 2-mm diameter flat-punch portable indenter, designed and assembled at the National Research Council of Canada (Boucherville, QC, Canada). The device was attached to a fixed arm above an elevated plate onto which the surgical sample was placed. Indentation measurements were performed by manually applying the device to an indentation depth of 2 mm. After excision of the brain tumor tissue, the specimens were placed in a saline solution at a temperature just $> 0^{\circ}C$ to limit structural changes to the tissue. Although the biomechanical properties of human brain tissue will not change substantially within the first 6 hours after resection, we transported the specimens to the pathology laboratory within 5 minutes, and the biomechanical measurements were started within 15 minutes after resection (Figure 1A).[21] Given the limitations of the portable indenter, only compressibility measurements could be conducted on the samples. The specimens were divided into quadrants using precut guides, and the measurements were repeated twice, with

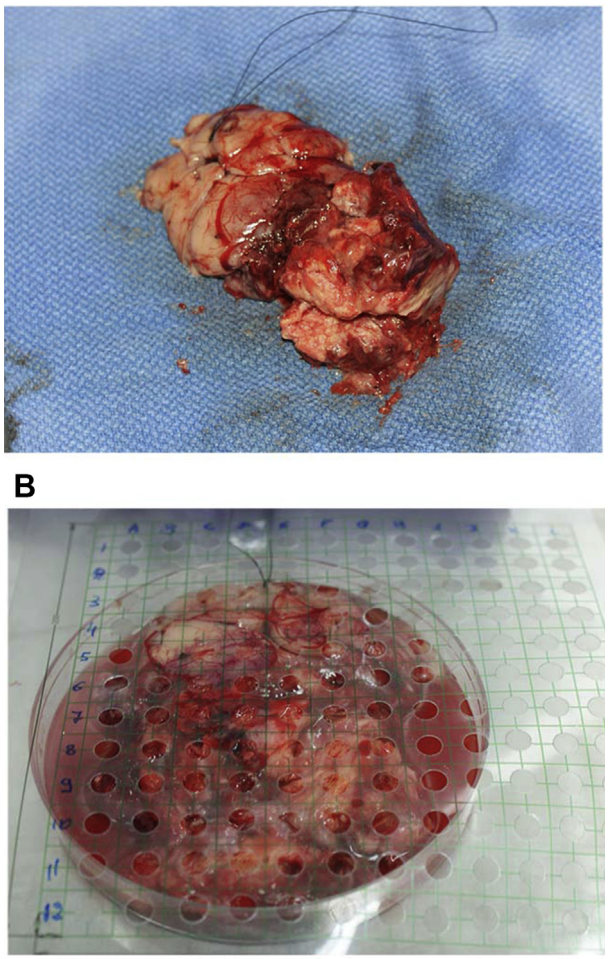

Figure 1. Primary human brain tumor specimens. (**A**) Primary human brain tumor with reference suture immediately after resection. (**B**) Primary human brain tumor with superimposed grid. Stiffness was measured by guiding the flat punch through the precut circular hole in the grid.

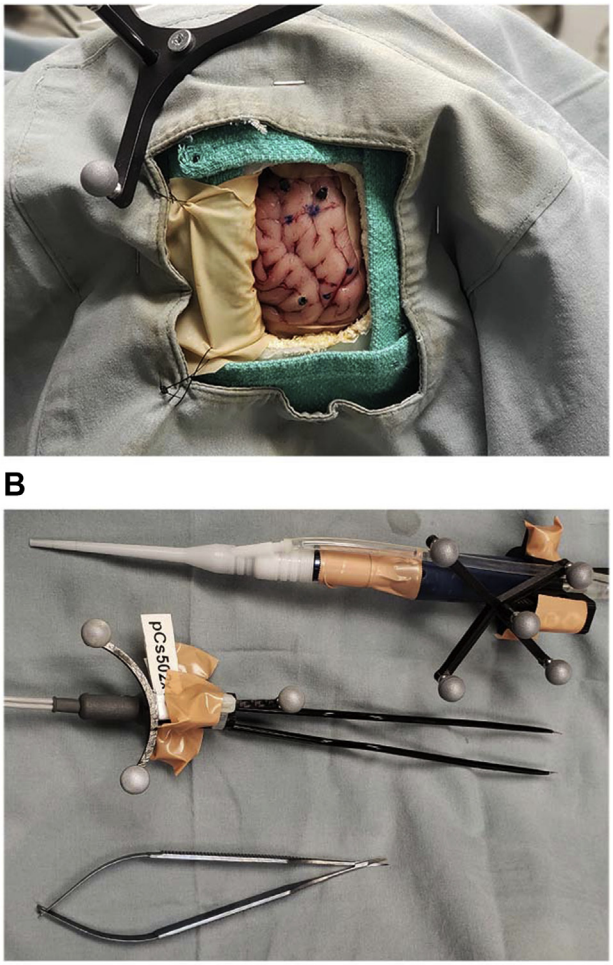

Figure 2. Operative view of artificial brain tumor and ex vivo calf brain. (**A**) Operative view of draped surgical field for ex vivo calf brain containing an alginate hydrogel artificial tumor. Ink on the brain surface outlines the limits of surgical resection. *Black spheres* represent tips of fiducial markers in the brain used to merge the pre- and postoperative images. (*Upper Left*) A fixed reference arm with fiducial markers can be seen. (**B**) Microscissors, ultrasonic aspirator, and bayonetted bipolar electrocautery device with custom 3-dimensional printed mounted fiducial markers to all for movement capture. Surgical tape was used to cover any reflective metal surfaces.

a final average computed between the 2 used (Figure 1B). After biomechanical characterization, the samples were sent to the pathology department for clinical assessment. The histopathological diagnosis of each specimen was obtained from the clinical pathological report. Any specimen results that were not confirmed to contain tumor were removed from the analysis.

Each patient whose tumor was used provided written informed consent for inclusion. The local University Health Centre Research Ethics Board, Neurosciences-Psychiatry, approved the present study to perform human tumor stiffness characterization.

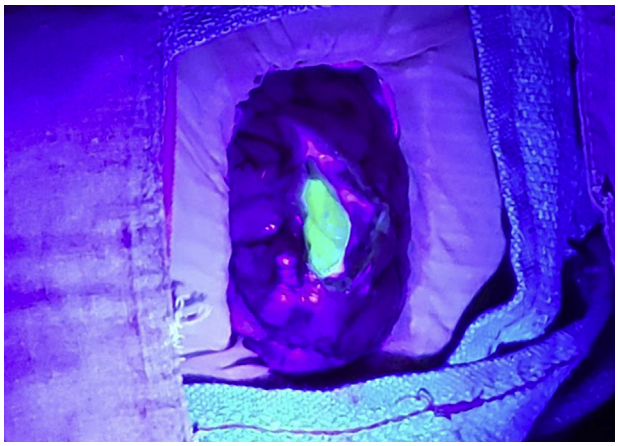

Figure 3. Photograph of an alginate tumor with incorporated florescent solution shown fluorescing under ultraviolet light. The cortical surface had been unroofed to allow for direct tumor visualization.

Artificial Tumor Development

The biomechanical properties of the hydrogel were characterized using the model HR-2 Rheometer (TA Instruments, New Castle, Delaware, USA). A time-sweep test was used to characterize the gelation kinetics of the gel. During such tests, the polymer system undergoes a solid–gel transition and solidifies into a solid-like gel, and its biomechanical property reaches a plateau (i.e., equilibrium state). Thus, the gelation process is irreversible and can be characterized using a single time-sweep test. As such, each testing session represented a new tumor, and no tumor was tested more than once.

A 2% weight by volume Algin I-1G Alginate (KIMICA Corp., Tokyo, Japan) served as the basis for the artificial tumor. Deionized water at room temperature was mixed with the requisite powder of alginate (kept in standard refrigeration for preservation purposes) and allowed to passively mix during a 3-day period until full dissolution in standard residential-grade refrigeration at 4°C. We chose to perform all biomechanical experiments within 1 week of alginate gel creation to avoid any potential degradation. The desired tumor stiffness was obtained by varying the input of calcium sulfate solution in the alginate–calcium sulfate mixture. To imitate the postgadolinium hyperintensity seen in many high-grade primary brain tumors, a 10-times dilution of gadolinium solution (Gadobutrol [Bayer AG, Leverkusen, Germany]) was added to the deionized water to reach a final concentration of 1 mM/L in the hydrogel. Tumor fluorescence under ultraviolet light was achieved by adding a fluorescein solution extracted from an "invisible ink" marker (iPang UV Light Pen [iPang Co., Ltd., South Korea]) to the deionized water.

The final composition of each 1100-µL tumor consisted of 1000 µL of 2% weight by volume alginate gel, 71 µL of deionized water with yellow and red coloring (Club House [McCormick & Co., Inc., Baltimore, Maryland, USA]), 13 µL of a 1-M concentration of calcium sulfate, 11 µL of a 100-µM gadolinium solution, and 5 µL

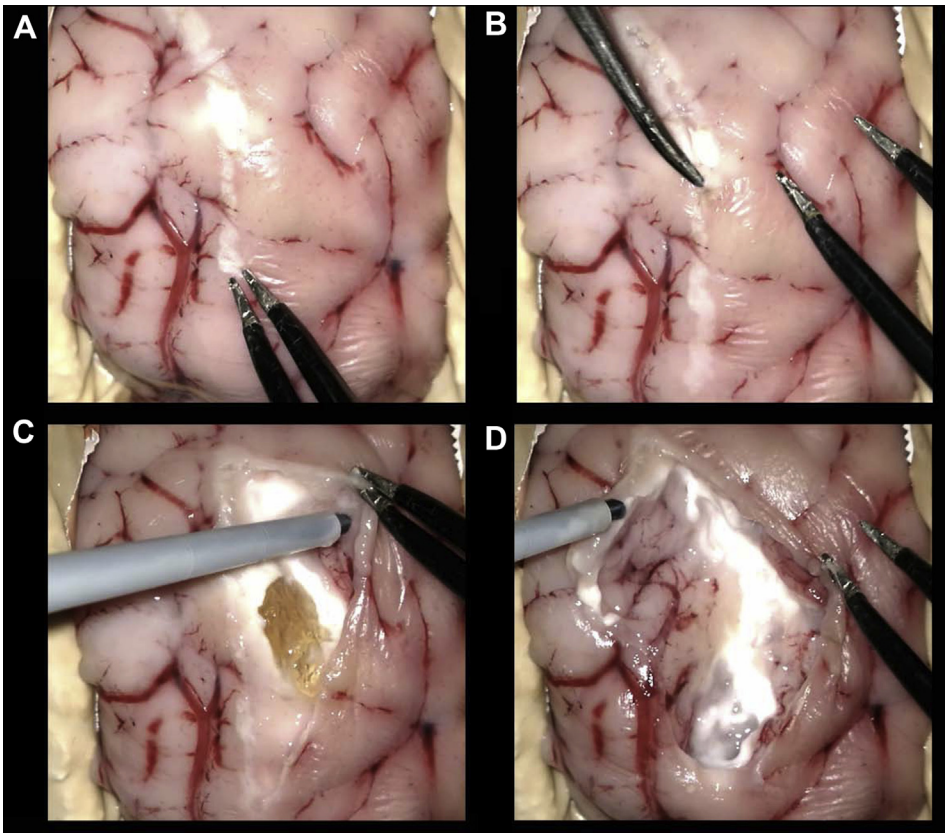

Figure 4. Resection of an alginate tumor implanted in an ex vivo calf brain as viewed through an operative microscope. (**A**) Pial coagulation with bipolar device. (**B**) Pial cutting using bayonetted microscissors. (**C**) Subpial technique performed with ultrasonic aspirator and bipolar device. Tumor shown in *yellow*. (**D**) Postoperative view demonstrating complete resection of tumor and gyrus with adjacent sulcal banks seen on either side. White matter can be seen deep in the cavity.

of fluorescein solution. This corresponded to a final calcium sulfate concentration of 12 mM within the hydrogel.

Ex Vivo Animal Brain

Cranially extricated, fresh calf brains were obtained. These were chosen because of their abundant availability, cost, size (~300 g; small enough to fit in an animal 7T MRI coil), and morphological similarity to the human brain.[22] Bovine simulation platforms have also been described for microsurgical training in neurosurgery.[2,23-25]

Alginate hydrogels were injected at a 30° angle at a subcortical depth of 5–7 mm in the longest continuous frontal gyrus, typically the second frontal gyrus. To provide a healthy margin for tumor solidification, we allowed 30 minutes to elapse before operation. The tumor was shaped by hydrodissection at the time of injection.

Video available at www.sciencedirect.com

The ex-vivo brain with the injected tumor was placed into a 3-dimensional (3D)-printed (Ultimaker S5 [Ultimaker, Utrecht, Netherlands]) form-fitted holder underneath a plastic cranium with a precut window to mimic an off-midline craniotomy view squared off with towels and drapes (Figure 2A). Microscissors, bipolar electrocautery, and an ultrasonic aspirator (Stryker, Kalamazoo, Michigan, USA) were available (Figure 2B). The incorporated fluorescein solution resulted in avid tumor fluorescence under ultraviolet black light (Figure 3). The operation was conducted in an animal operative suite equipped with an OPMI Pico surgical microscope (Carl Zeiss Co., Oberkochen, Germany). To record the operation, high-density multimedia interface outputs from the microscope and a ceiling mounted camera were routed through a high-density multimedia interface recording device (HDML-Cloner box turbo HCB-988BT [Cloner Alliance Inc., Hong Kong, China]). A sample operation of a subpial resection technique can be viewed in Supplementary Video 1, with key images shown in Figure 4.

Imaging Characteristics of Artificial Tumor on MRI and Ultrasonography

MRI was performed using the 7T Bruker Pharmascan (Bruker Biosciences, Billerica, Massachusetts, USA) ultra-high-field system. The brains were housed in a cylindrical container and

Table 1. Biomechanical Properties of Human Primary Brain Tumors

Object	Force (kPa)	
	Mean ± SD (Range)	Median (IQR)
Human brain tumor		
DNET ($n = 1$)	3.31 ± 1.35 (1.81–6.61)	2.86 (2.80–3.27)
Oligodendroglioma ($n = 2$)	6.74 ± 6.82 (1.14–23.07)	1.95 (1.52–12.51)
Anaplastic astrocytoma ($n = 1$)	1.37 ± 0.67 (0.50–2.38)	1.34 (0.72–1.88)
Glioblastoma ($n = 3$)	4.14 ± 2.68 (0.44–9.85)	2.93 (2.36–5.98)
Alginate hydrogel		
Calcium 10 µL ($n = 7$)	2.01 ± 0.75 (1.08–3.18)	2.22 (1.14–2.46)
Calcium 11 µL ($n = 9$)	2.85 ± 0.72 (1.80–3.90)	2.88 (2.43–3.27)
Calcium 12 µL ($n = 4$)	2.24 ± 0.64 (1.80–3.18)	1.98 (1.83–2.64)

SD, standard deviation; IQR, interquartile range; DNET, dysembryoplastic neuroepithelial tumor.

immersed in an MRI-invisible fluorinated solution (FC-40 [Sigma-Aldrich, St. Louis, Missouri, USA]) to remove the background MRI signal. For radiofrequency excitation and reception, a 6-cm inner diameter volume resonator was used. The imaging protocol included a 3D steady-state free precession MRI sequence with an echo time of 5 ms, repetition time of 10 ms, a receiver bandwidth of 50 kHz, and an excitation pulse flip angle of 30°. The image acquisition matrix was selected to achieve an isotropic voxel resolution of 150 µm initially. However, after 4 trials, the resolution was reduced to 200 µm to decrease the scanning time. The field of view size was adjusted according to the position of the calf brain within the container. However, the voxel resolution remained constant for all samples. We collected 24 signal averages, for a total scan time of ~12 hours per sample for the overnight histology-grade scan. To assist in alignment of the pre- and postoperative images, plastic reference arrays were inserted into the brain at the margins of the craniotomy. Tumor enhancement was achieved by incorporating gadobutrol (Bayer AG, Leverkusen, Germany) in the tumor.

Ultrasound images of the tumor were also acquired using an HDI 5000 ultrasound scanner with a phased array probe (P4-7 [Philips, Amsterdam, Netherlands]). The probe spatial position in relation to a fixed reference tool was obtained using the IBIS (intraoperative brain imaging system) neuronavigation system,[26] with an optical tracking camera (Polaris [Northern Digital Inc., Waterloo, Ontario, Canada]).

Surgical Movement Capture

Fiducial markers (Northern Digital Inc.) were attached to the bipolar electrocautery device and ultrasonic aspirator via custom 3D-printed polylactic acid mounts. An optical tracking camera (FusionTrack 500 [Atracsys LLC, Puidoux, Switzerland]) was used to capture the movement of the bipolar electrocautery device and ultrasonic aspirator with reference to the fixed fiducial markers mounted adjacent to the craniotomy window.

Statistical and Imaging Analysis

The descriptive statistics are reported as counts and percentages for the categorical variables. For normally distributed continuous variables, the mean ± standard deviation is reported. Data analysis and visualization were conducted using Stata Statistical Software, release 13 (StataCorp, College Station, Texas, USA) and MATLAB, Statistics Toolbox, release 2017b (MathWorks, Inc., Natick, Massachusetts, USA), respectively. Ultrasonography and MRI postprocessing were completed using an open-source software application framework, 3D Slicer, version 4.10.01.[27]

RESULTS

Mechanical Properties of Human Primary Brain Tumors

A total of 68 tumor stiffness measurements were conducted on 8 patient samples. The biomechanical properties of these groups are listed in Table 1.

Mechanical Properties of Artificial Tumor Compared with Primary Human Brain Tumors

Rheology was performed on the pure alginate and calcium sulfate mixtures. We conducted 24 rheometer testing sessions, each lasting 1 hour. Of the 24 sessions, 4 were excluded because of erroneous signals during testing, either from accidental contact with the rheometer probe or slow transfer of the alginate mixture onto the rheometer. The hydrogels had reached a maximum stiffness within a mean of 81 seconds (range, 36–130 seconds). For ease of analysis when comparing the hydrogel stiffness, the brain tumors were divided into 2 groups: glioblastoma ($n = 3$) and all others ($n = 4$). The biomechanical properties of the various hydrogel concentrations in relationship to the primary brain tumor groups are listed in Table 1. Owing to the skewed nature of the data, a Kruskal-Wallis test was used to compare the stiffness of the tumor groups with the 10-, 11-, and 12-mM concentrations of alginate hydrogel. No significant differences were found between any of the groups [$\chi^2(4) = 9.187$; $P = 0.057$].

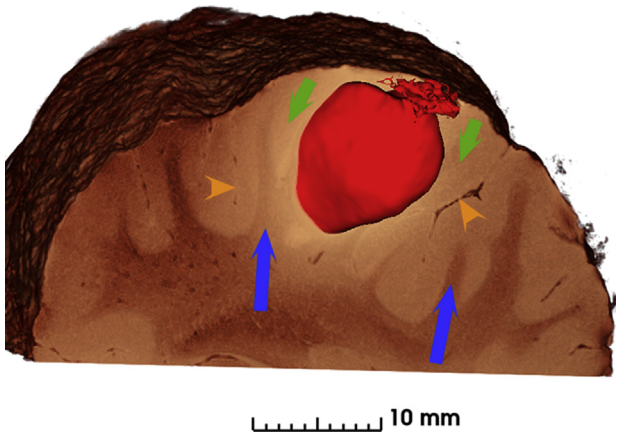

Figure 5. Magnetic resonance image (7T) of alginate hydrogel tumor (red) in an ex vivo calf brain. Long blue arrows indicate white matter; medium green arrows indicate gray matter; and short orange arrows indicate sulci.

Imaging Tumor Characteristics

The tumor and surrounding brain architecture were well identified on MRI (Figure 5). MRI and ultrasound image registration allowed for ease of identification of the tumor on the MRI and ultrasound scans (Figure 6). Using the 3D Slicer with Otsu thresholding and segmentation, the hyperintense tumor and gray and white matter could be quantified in 0.003-mm^3 increments.

Surgical Movement Capture

The movement data of the instruments were successfully captured (Figure 7) and transformed into performance metrics using techniques previously described in neurosurgical virtual reality surgery.[28-31] In a recent report, 270 performance metrics were generated from a virtual reality simulator neurosurgical tumor resection task.[32] Given the near-infinite number of metrics that could be generated from digitized data, we limited the number of metrics generated to a select few to highlight the potential of this technology. The mean aspirator and bipolar velocity were 16.8 mm/second and 11.35 mm/second, respectively. The mean aspirator and bipolar acceleration were 7.81 mm/s^2 and 5.21 mm/s^2, respectively. The mean instrument tip distance was 9.95 mm.

DISCUSSION

We have developed a comprehensive research framework that allows for the study of technical performance and extent of resection in oncological neurosurgery. This platform relies on a cost-effective alginate-based artificial brain tumor incorporated into an ex-vivo calf brain within a controlled operative environment. To the best of our knowledge, this represents the first instance in which an artificial tumor was created based on the biomechanical properties of human specimens obtained at resection.

The overall cost of the artificial tumor is well under 2 cents/mL, given that its elements are relatively inexpensive and combined in small quantities. To put this in perspective, 1 kg of alginate and calcium sulfate can yield 40,000 and 5800 mL of final tumor, respectively. Gadobutrol (Bayer AG), or its analogues, arguably the most expensive compound in the mixture, can often be obtained at minimal cost from expired stockpiles kept in clinical units. Even if one were to pay the full cost for an average 30-mL vial, this would yield 27,000 mL of tumor. Access to a 10–100-µL pipette and laboratory-grade scale are required, but remain one-time purchases.

Operative "performance" can be assessed both from the recordings from the surgical microscope and ceiling-mounted camera and from the movements generated from the instrument-mounted fiducial markers. Although no standardized method of evaluating surgical movement exists, the results from the present study have demonstrated that raw fiducial movement data can be successfully transformed into performance metrics.

The extent of resection can be assessed via a number of modalities. Ultraviolet fluorescence remains an imprecise, albeit cost-effective, method of detecting residual tumor. In contrast, ultrasonography can allow for more precise quantification of residual disease during and at completion of the procedure. Using tumor margins were redily identified using the HDI 5000 ultrasound scanner with a P4-7 probe, with an image resolution of 0.23 mm × 0.23 mm. In addition, MRI is sensitive to contrast enhancement. It is also more sensitive to the precise volume of resected tumor, gray matter, and white matter tissue. Moreover, the high spatial resolution (200-µm isotropic voxel sizes) of the ex-vivo 7-T MRI scans present an opportunity for more accurate quantification of the operative outcome.

Extensive work has been done to create meaningful surgical performance measures from raw movement data in virtual reality neurosurgery, ranging from simple, user-generated metrics[28-31] and 3D representations of movement and force[33,34] to artificial intelligence-assisted methods.[32,35,36] Similar analyses of live surgical movement in an experimental or clinical environment might allow for a better understanding of surgical nuance, technical expertise, and complication avoidance.

The development of simulation platforms such as the NeuroVR (formerly NeuroTouch [CAE Healthcare, Montreal, Quebec, Canada]) have made it possible to better understand the technical composites required to carry out intra-axial tumor resection.[37] By allowing for the creation of complex tumor resection scenarios and integrating the physical properties of human brain tumors obtained at resection, the NeuroVR (CAE Healthcare) provides the most realistic computer-based recapitulation of oncological neurosurgery to date.[38]

Face, content, and construct validity for the NeuroVR (CAE Healthcare) have been demonstrated.[28-31] However, the question of concurrent validity (i.e., whether practice on the simulator improves performance in the "real world") would be best addressed by conducting a randomized controlled trial. However, the significant variability resulting from differences in pathology, patient factors, unpredictability of the operating room environment, and multiple surgeon input confounds the relationship between a surgical act and patient outcome and serves to decrease statistical power. Although a reduction in power can traditionally be addressed by increasing the number of recruits, notwithstanding the extra resources that might require, the operative setting presents ethical concerns for patient safety when experimental interventions are involved. A research ethics board might

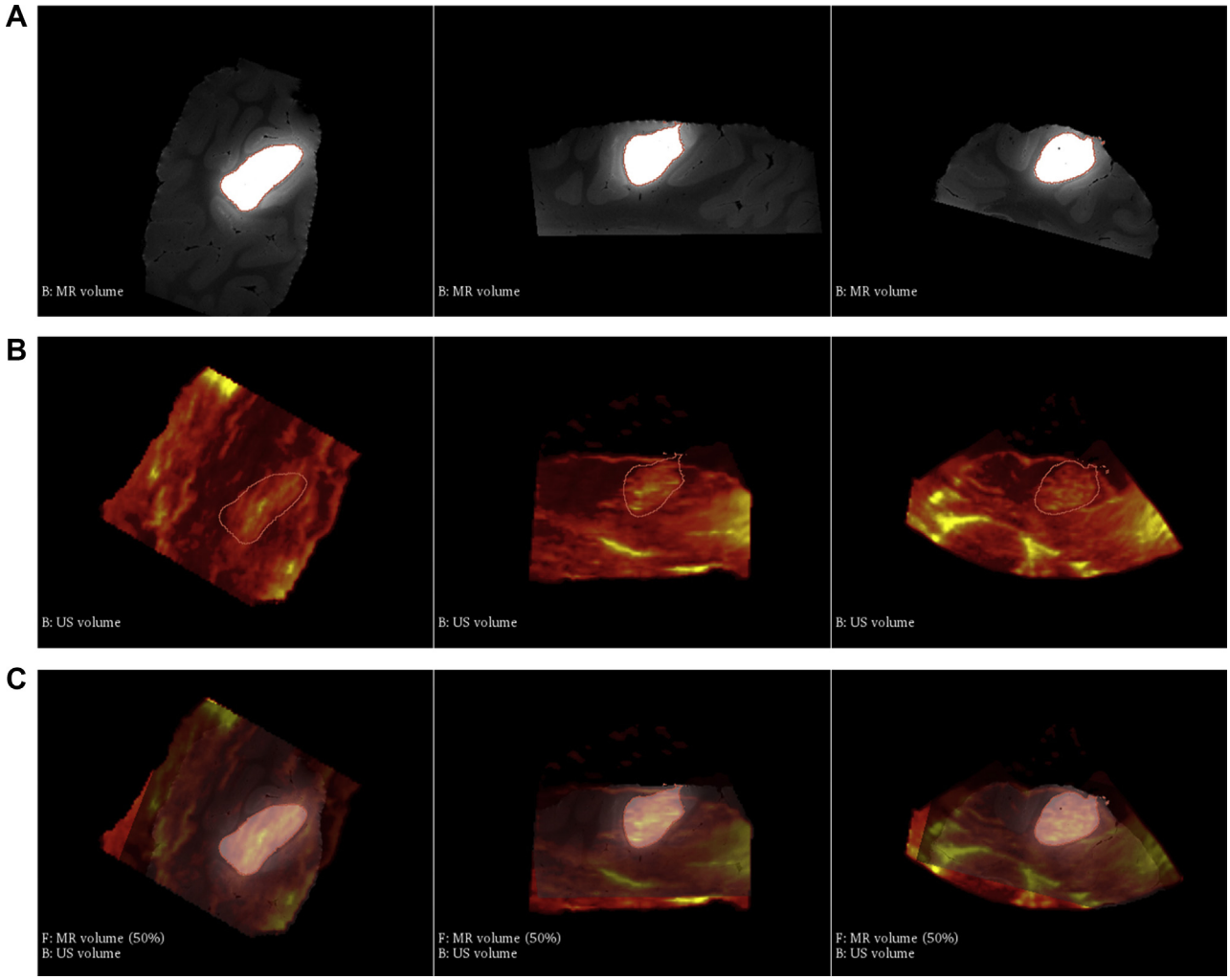

Figure 6. A comparison of magnetic resonance images and ultrasound images of the alginate hydrogel tumor in an ex vivo calf brain. Sagittal, axial, and coronal views of the hyperintense alginate hydrogel tumor in ex vivo calf brain on (**A**) 7T magnetic resonance images, (**B**) ultrasound images, and (**C**) both overlaid. Tumor hyperintensity was achieved by incorporating gadolinium solution into the hydrogel tumor. The *red outline* of the tumor was added via postprocessing in 3D Slicer and visualized using IBIS (intraoperative brain imaging system).

question the existence of equipoise in a study comparing traditional residency training (control group) with traditional residency training in addition to virtual reality operative rehearsal (experimental group). Additionally, the residents who might most benefit from operative rehearsal could be at a stage in their training at which they could not yet safely conduct oncological neurosurgery with minimal supervisor assistance.

If successful, the proposed randomized controlled trial would be the first time simulated operative rehearsal has been demonstrated to influence surgical performance in an open neurosurgical procedure. Surgical "boot camps" involving simulators have already been developed for trainees early in neurosurgical residency.[39,40] These residents, early in their learning curve, stand to benefit the most from the experiential training afforded by simulators,[41] and one could envision that residency programs, hospital administrators, and patient advocacy groups would require simulation training as a mandatory precursor to participation in high-risk operative cases early in training. Ultimately, standardizing surgical education and training to an expert level, rather than competency, has the potential to reduce operative complications, leading to decreased patient morbidity and mortality and reduced medical care costs.

Study Limitations

Unless the preparations have been performed in sterile environments, bacterial contamination can occur, which can lead to biomechanical inconsistency of the gel beyond 2 weeks. Approaches to sterilize the alginate, like sterile filtration have been well established in reported studies but were not pursued in the present study. Three days between alginate gel creation and its use

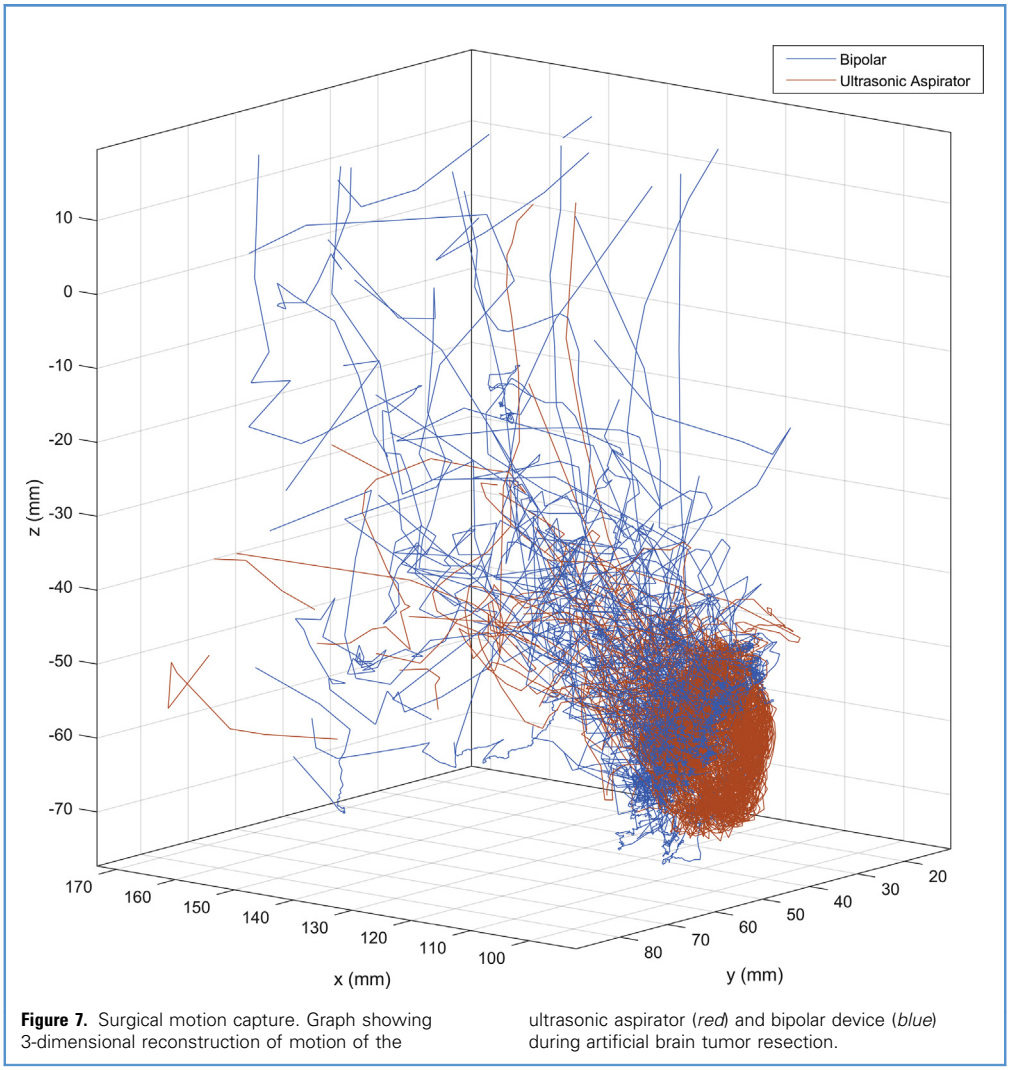

Figure 7. Surgical motion capture. Graph showing 3-dimensional reconstruction of motion of the ultrasonic aspirator (*red*) and bipolar device (*blue*) during artificial brain tumor resection.

is required; therefore, some foresight is necessary to integrate its use in a clinical or educational context.

The neovascularization inherent to many primary brain tumors makes achieving adequate hemostasis during surgery an important aspect of training. Although we achieved intracranial and capillary blood flow using a porcine brain,[42,43] with cannulated carotid arteries as described in human cadaveric studies,[44] that animal model had significant limitations. The thick skull and relatively small brain volume made surgical access time-consuming and inefficient.[45] Furthermore, the large porcine head could not fit inside the 7T MRI coil, and removing the brain to allow for accurate scanning risked damaging the tissue. Therefore, we decided to use calf brain, despite the fact that this model has no active bleeding state.

Although no limitations exist regarding where the tumor can be injected into the calf brain, in the present study, we emphasized cortically-based primary tumors. Deep-seated lesions add an extra dimension of difficulty, which can be explored in the future. Furthermore, the hydrodissection caused by tumor injection into the brain prevents the creation of the indistinct brain—tumor border characteristic of primary brain tumors. The ex-vivo nature of the model does not allow for the development of reactive gliosis (and the resulting subtle biomechanical changes) surrounding the tumor familiar to neurosurgeons. Ideally, tumors injected into live animals should be given time to develop a reactive gliosis; however, the challenges and ethical concerns in maintaining animals during this period are substantial.

The operative outcomes have been defined purely in imaging terms. Although the ex-vivo nature of the brain samples precluded a functional assessment, the extent of subcortical white matter injury might provide a useful imaging correlate, as some have suggested.[46]

Insights from crew resource management in aviation have stressed the importance of group training in high-stress, technically demanding environments that require the cooperation of numerous individuals.[47] As such, although the present study did not include an assistant surgeon or nurse, the current framework can easily integrate additional team members.

CONCLUSIONS

A comprehensive research framework to study operative expertise in oncological intracranial neurosurgery has been developed. This framework can offer clinicians, students, and researchers the ability to perform operative rehearsal, teaching, and studies involving intraparenchymal brain tumor surgery in a controlled laboratory environment and represents a crucial step in the understanding and training of expertise in neurosurgery.

CRediT AUTHORSHIP CONTRIBUTION STATEMENT

Alexander Winkler-Schwartz: Conceptualization, Methodology, Formal analysis, Investigation, Resources, Writing - original draft, Writing - review & editing, Visualization, Project administration, Funding acquisition. **Recai Yilmaz:** Methodology, Validation, Formal analysis, Investigation, Writing - review & editing. **Dan Huy Tran:** Methodology, Investigation, Writing - review & editing. **Houssem-Eddine Gueziri:** Software, Visualization. **Binbin Ying:** Methodology, Resources, Writing - review & editing. **Marius Tuznik:** Investigation, Data curation, Writing - review & editing. **Vladimir Fonov:** Software, Writing - review & editing. **Louis Collins:** Conceptualization, Methodology, Software, Writing - review & editing, Funding acquisition. **David A. Rudko:** Methodology, Investigation, Resources, Writing - review & editing, Supervision. **Jianyu Li:** Conceptualization, Methodology, Writing - review & editing. **Patricia Debergue:** Methodology, Validation, Formal analysis, Investigation, Writing - review & editing. **Valerie Pazos:** Methodology, Validation, Formal analysis, Investigation, Writing - review & editing. **Rolando Del Maestro:** Conceptualization, Methodology, Resources, Supervision, Funding acquisition.

REFERENCES

1. Aurich LA, Silva Junior LF, Monteiro FM, Ottoni AN, Jung GS, Ramina R. Microsurgical training model with nonliving swine head: alternative for neurosurgical education. *Acta Cir Bras*. 2014;29:405-409.
2. Turan Suslu H, Ceylan D, Tatarli N, et al. Laboratory training in the retrosigmoid approach using cadaveric silicone injected cow brain. *Br J Neurosurg*. 2013;27:812-814.
3. Oliveira MM, Araujo AB, Nicolato A, et al. Face, content, and construct validity of brain tumor microsurgery simulation using a human placenta model. *Oper Neurosurg*. 2015;12:61-67.
4. Ashour AM, Elbabaa SK, Caputy AJ, Gragnaniello C. Navigation-guided endoscopic intraventricular injectable tumor model: cadaveric tumor resection model for neurosurgical training. *World Neurosurg*. 2016;96:261-266.
5. Berhouma M, Baidya NB, Ismail AA, Zhang J, Ammirati M. Shortening the learning curve in endoscopic endonasal skull base surgery: a reproducible polymer tumor model for the transsphenoidal trans-tubercular approach to retroinfundibular tumors. *Clin Neurol Neurosurg*. 2013;115:1635-1641.
6. Gragnaniello C, Nader R, van Doormaal T, et al. Skull base tumor model. *J Neurosurg*. 2010;113:1106-1111.
7. Kamp MA, Knipps J, Steiger H-J, et al. Training for brain tumour resection: a realistic model with easy accessibility. *Acta Neurochir (Wien)*. 2015;157:1975-1981.
8. Mashiko T, Oguma H, Konno T, et al. Training of intra-axial brain tumor resection using a self-made simple device with agar and gelatin. *World Neurosurg*. 2018;109:e298-e304.
9. Valli D, Belykh E, Zhao X, et al. Development of a simulation model for fluorescence-guided brain tumor surgery. *Front Oncol*. 2019;9:748.
10. Csokay A, Papp A, Imreh D, Czabajszky M, Valalik I, Antalfi B. Modelling pathology from autolog fresh cadaver organs as a novel concept in neurosurgical training. *Acta Neurochir (Wien)*. 2013;155:1993-1995.
11. Chen SJ, Hellier P, Marchal M, et al. An anthropomorphic polyvinyl alcohol brain phantom based on Colin27 for use in multimodal imaging. *Med Phys*. 2012;39:554-561.
12. Chen SJ, Hellier P, Gauvrit JY, Marchal M, Morandi X, Collins DL. An anthropomorphic polyvinyl alcohol triple-modality brain phantom based on Colin27. *Med Image Comput Comput Assist Interv*. 2010;13(Pt 2):92-100.
13. Reinertsen I, Collins DL. A realistic phantom for brain-shift simulations. *Med Phys*. 2006;33:3234-3240.
14. Lee J-S, Tailor A-RA, Lamki T, Zhang J, Ammirati M. Properties and storage methods of the Stratathane ST-504—based neurosurgical tumor model: comprehensive analysis. *World Neurosurg*. 2016;96:350-354.
15. Gragnaniello C, Gagliardi F, Chau AMT, et al. Intracranial injectable tumor model: technical advancements. *J Neurol Surg Part B*. 2014;75:301-308.
16. Stewart DC, Rubiano A, Dyson K, Simmons CS. Mechanical characterization of human brain tumors from patients and comparison to potential surgical phantoms. *PLoS One*. 2017;12:e0177561.
17. Lee KY, Mooney DJ. Alginate: properties and biomedical applications. *Prog Polym Sci*. 2012;37:106-126.
18. Li J, Weber E, Guth-Gundel S, et al. Tough composite hydrogels with high loading and local release of biological drugs. *Adv Healthcare Mater*. 2018;7:1701393.
19. Rowley JA, Madlambayan G, Mooney DJ. Alginate hydrogels as synthetic extracellular matrix materials. *Biomaterials*. 1999;20:45-53.
20. Zhao X, Huebsch N, Mooney DJ, Suo Z. Stress-relaxation behavior in gels with ionic and covalent crosslinks. *J Appl Phys*. 2010;107:63509.
21. Garo A, Hrapko M, Van Dommelen J, Peters G. Towards a reliable characterisation of the mechanical behaviour of brain tissue: the effects of post-mortem time and sample preparation. *Biorheology*. 2007;44:51-58.
22. Schmidt MJ, Pilatus U, Wigger A, Kramer M, Oelschläger HA. Neuroanatomy of the calf brain as revealed by high-resolution magnetic resonance imaging. *J Morphol*. 2009;270:745-758.
23. Gökyar A, Cokluk C. Using of fresh cadaveric cow brain in the microsurgical training model for sulcal-cisternal and fissural dissection. *J Neurosci Rural Pract*. 2018;9:26-29.
24. Hicdonmez T, Hamamcioglu MK, Tiryaki M, Cukur Z, Cobanoglu S. Microneurosurgical training model in fresh cadaveric cow brain: a laboratory study simulating the approach to the circle of Willis. *Surg Neurol*. 2006;66:100-104 [discussion: 104].
25. Hicdonmez T, Hamamcioglu MK, Parsak T, Cukur Z, Cobanoglu S. A laboratory training model for interhemispheric-transcallosal approach to the lateral ventricle. *Neurosurg Rev*. 2006;29:159-162.
26. Drouin S, Kochanowska A, Kersten-Oertel M, et al. IBIS: an OR ready open-source platform for image-guided neurosurgery. *Int J Comput Assist Radiol Surg*. 2017;12:363-378.
27. Fedorov A, Beichel R, Kalpathy-Cramer J, et al. 3D Slicer as an image computing platform for the quantitative imaging network. *Magn Reson Imaging*. 2012;30:1323-1341.
28. Alotaibi FE, AlZhrani GA, Sabbagh AJ, Azarnoush H, Winkler-Schwartz A, Del Maestro RF. Neurosurgical assessment of metrics including judgment and dexterity using the virtual reality simulator NeuroTouch (NAJD Metrics). *Surg Innov*. 2015;22:636-642.
29. Alotaibi FE, AlZhrani GA, Mullah MA, et al. Assessing bimanual performance in brain tumor resection with NeuroTouch, a virtual reality simulator. *Neurosurgery*. 2015;11(suppl 2):89-98 [discussion: 98].
30. Winkler-Schwartz A, Bajunaid K, Mullah MA, et al. Bimanual psychomotor performance in neurosurgical resident applicants assessed using NeuroTouch, a virtual reality simulator. *J Surg Educ*. 2016;73:942-953.

31. AlZhrani G, Alotaibi F, Azarnoush H, et al. Proficiency performance benchmarks for removal of simulated brain tumors using a virtual reality simulator NeuroTouch. *J Surg Educ*. 2015;72:685-696.

32. Winkler-Schwartz A, Yilmaz R, Mirchi N, et al. Machine learning identification of surgical and operative factors associated with surgical expertise in virtual reality simulation. *JAMA Network Open*. 2019;2:e198363.

33. Sawaya R, Bugdadi A, Azarnoush H, et al. Virtual reality tumor resection: the force pyramid approach. *Oper Neurosurg (Hagerstown)*. 2018;14:686-696.

34. Azarnoush H, Siar S, Sawaya R, et al. The force pyramid: a spatial analysis of force application during virtual reality brain tumor resection. *J Neurosurg*. 2017;127:171-181.

35. Bissonnette V, Mirchi N, Ledwos N, et al. Artificial intelligence distinguishes surgical training levels in a virtual reality spinal task. *J Bone Joint Surg Am*. 2019;101:e127.

36. Siyar S, Azarnoush H, Rashidi S, et al. Machine learning distinguishes neurosurgical skill levels in a virtual reality tumor resection task. *Med Biol Eng Comput*. 2020;58:1357-1367.

37. Delorme S, Laroche D, DiRaddo R, Del Maestro RF. NeuroTouch: a physics-based virtual simulator for cranial microneurosurgery training. *Neurosurgery*. 2012;71:ONS32-ONS42.

38. Sabbagh AJ, Bajunaid KM, Alarifi N, et al. Roadmap for developing complex virtual reality simulation scenarios: the subpial neurosurgical tumor resection model. *World Neurosurg*. 2020;139:e220-e229.

39. Haji FA, Clarke DB, Matte MC, et al. Teaching for the transition: the Canadian PGY-1 neurosurgery "rookie camp". *Can J Neurol Sci*. 2015;42:25-33.

40. Harrop J, Lobel DA, Bendok B, Sharan A, Rezai AR. Developing a neurosurgical simulation-based educational curriculum: an overview. *Neurosurgery*. 2013;73(suppl 1):25-29.

41. Sadideen H, Kneebone R. Practical skills teaching in contemporary surgical education: how can educational theory be applied to promote effective learning? *Am J Surg*. 2012;204:396-401.

42. Regelsberger J. Surgery of the brain and spinal cord in a porcine model. In: Janowski M, ed. *Experimental Neurosurgery in Animal Models*. New York, NY: Humana Press; 2016:165-173.

43. Regelsberger J, Eicker S, Siasios I, et al. In vivo porcine training model for cranial neurosurgery. *Neurosurg Rev*. 2015;38:157-163 [discussion: 163].

44. Aboud E, Al-Mefty O, Yaşargil MG. New laboratory model for neurosurgical training that simulates live surgery. *J Neurosurg*. 2002;97:1367-1372.

45. Sauleau P, Lapouble E, Val-Laillet D, Malbert CH. The pig model in brain imaging and neurosurgery. *Animal*. 2009;3:1138-1151.

46. Duffau H, Peggy Gatignol ST, Mandonnet E, Capelle L, Taillandier L. Intraoperative subcortical stimulation mapping of language pathways in a consecutive series of 115 patients with grade II glioma in the left dominant hemisphere. *J Neurosurg*. 2008;109:461-471.

47. Bradley P. The history of simulation in medical education and possible future directions. *Med Educ*. 2006;40:254-262.

Conflict of interest statement: Stryker provided surgical instrument loans in the form of a Sonopet ultrasonic aspirator, bipolar electrocautery, and handheld drill system; however, the company had no role in the content of the present study.

Portions of the present study were presented in poster form during the proceedings at the Congress of Neurological Surgeons Annual Meeting, San Francisco, October 22, 2019.

Received 26 May 2020; accepted 28 July 2020

Citation: World Neurosurg. (2020) 144:e62-e71.
https://doi.org/10.1016/j.wneu.2020.07.209

Journal homepage: ***www.journals.elsevier.com/world-neurosurgery***

Available online: ***www.sciencedirect.com***